DESIGN SENSITIVITY ANALYSIS OF HIGH-FREQUENCY STRUCTURAL ACOUSTIC PROBLEMS

Nam H. Kim[*], Jun Dong[§], and Kyung K. Choi[¶]

Department of Mechanical Engineering
University of Florida
PO Box 116300
Gainesville, FL 32611-6300

ABSTRACT

A design sensitivity formulation for structural–acoustic problems at high frequencies (1,000–20,000 Hz) is presented using the energy finite element method. The material property, panel thickness, and structural damping factor are taken as design variables. The continuum method is used to derive the design sensitivity equation of the energy flow equation, while the discrete method is used to calculate the variation of the coupling relation. The design variable's effect on the power transfer coefficient is discussed in detail. Even when the system matrix equation is not symmetric, the adjoint problem is solved using the same factorized matrix from energy finite element analysis. Design sensitivity results calculated from the proposed method are compared to finite difference sensitivity results with good agreement.

KEYWORDS

Energy Flow Analysis, Energy Finite Element Method, Design Sensitivity Analysis, Optimization

1. INTRODUCTION

Some research has been performed in structural–acoustic design using finite element and boundary element methods[1–5]. The continuum method, discrete method, and semi-analytical method are used to calculate design sensitivity. However, the practicality of these methods is limited to low frequency (20 – 200 Hz) design problems since an excessive number of elements are required in high frequency analysis.[6] The element size of the structural and acoustic domain must be smaller than the wavelength to ensure an accurate prediction.

* Assistant Professor, Member AIAA

§ Research Assistant, Center for Computer-Aided Design, University of Iowa, Iowa City, IA 52242

¶ Professor and Director, Associate Fellow AIAA, Center for Computer-Aided Design, University of Iowa, Iowa City, IA 52242

Since the response is very sensitive to small changes in the model at high frequencies, statistical energy analysis is often used to simulate the structural–acoustic behavior of a large system.[7–9] Given its similarities to the heat transfer problem, this approach uses the conservation of vibration energy within a subsystem of similar modes. From a design point of view, however, since a single energy value represents the lumped subsystem's status, the energy variation within a subsystem cannot be represented. In addition, the geometric and material parameters, which often serve as design variables, do not appear explicitly in the governing equation.

In contrast to statistical energy analysis, energy flow analysis has been developed using an analytical method that can represent the vibration behavior of a structure in the averaged sense.[10–13] The near–field response is disregarded in high frequency ranges, and the far–field response is used to represent the vibration behavior of the structure. Since energy conservation is imposed locally, it is possible to represent the structural geometry in detail, which is critical from a design point of view. Even if the response variable (energy density) is not continuous across structural junctions, this approach has been integrated with the finite element method to simulate the vibration behavior of a complicated structure at high frequencies.[6, 14–16]

Although energy flow analysis has been applied to engineering applications using the finite element method, its design sensitivity analysis and optimization has not been fully developed. In this paper, a rigorous development of design sensitivity analysis for the structural–acoustic energy flow problem is presented. The variational equation is differentiated with respect to design variables. Such design variables as the material property, panel thickness, and structural damping factor are taken into account, which are all parametric design variables, since the structural configuration does not change during the design process. The continuum method is used to derive the design sensitivity equation of the energy flow equation, while the discrete method is used to calculate the variation of the coupling relation. The design variable's effect on the power transfer coefficient is discussed in detail.

Two methods are proposed to calculate structural–

American Institute of Aeronautics and Astronautics

acoustic design sensitivity: the direct differentiation and the adjoint variable method. The former solves for response variable sensitivity and performance sensitivity is then obtained using the chain rule of differentiation. In contrast, the latter computes performance sensitivity by solving the adjoint problem. Even when the adjoint problem is not symmetric, the adjoint variable method still uses the same factorized coefficient matrix from response analysis. It is also shown that the adjoint problem is identical for different design variables. Design sensitivity results calculated from the proposed method are compared to finite difference sensitivity results with good agreement.

In energy flow analysis, the complicated geometry (built–up structures) is assembled from such simple structural components as rod, beam, membrane, plate, etc. by using the power transfer coefficient between components. This coefficient is a function of the design variables. Thus, in design sensitivity analysis it is necessary to derive the expression of the power transfer coefficient in terms of the design variables. Several methods are proposed to calculate the power transfer coefficient: analytical, artificial damping, and iterative. In this paper, an analytical method is chosen to calculate the power transfer coefficient and its sensitivity, since the last two methods present difficulties when used for design sensitivity calculation purposes.

2. ENERGY FLOW ANALYSIS

In order to develop a design sensitivity formulation in the subsequent section, energy flow analysis[6,12,13] and energy finite element analysis[6,14,15] are first reviewed, including a method to calculate the power transfer coefficient.

The energy flow equation for the steady–state structural–acoustic problem can be obtained through the energy conservation relation and the time– and space–averaging process[13] as

$$-\frac{c_g^2}{\eta\omega}\nabla^2 e + \eta\omega e = \pi \tag{1}$$

where e is the time– and space–averaged energy density function, η is the hysteresis–damping factor, ω is the excitation frequency, π is the input power density, and c_g is the group speed.[18] Note that the hysteresis–damping factor η is assumed to be small in the derivation of (1), i.e., $\eta \ll 1$.

As discussed by Cho and Bernhard,[14] the energy flow equation (1) satisfies within a structural component. Unlike displacement in structural problems, energy density e is not continuous across the junction between structural components. The connection between different components can be achieved through the conservation of power flow and the superposition of vibration energy. Consider a built–up structure made up of a collection of structural components. Each component occupies a domain Ω_i ($\subset R^2$) with boundary Γ_i ($i = 1,\ldots,r$). These domains are interconnected by constraints at each boundary; that is, structural components are connected to adjacent components by junctions that constrain admissible fields.
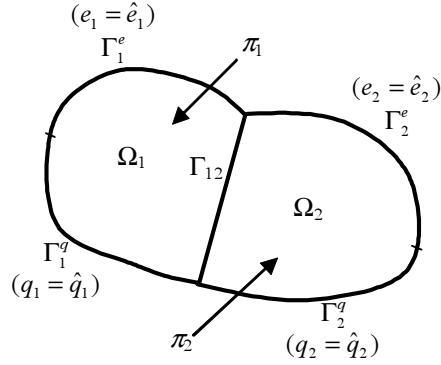

Figure 1 Built–up Structure with Components Ω_1 and Ω_2

Figure 1 illustrates a simple built–up structure with two components Ω_1 and Ω_2. The boundary of Ω_i is composed of: Γ_i^e where the energy density e is prescribed, Γ_i^q where the power flow q is prescribed, and the junction boundary Γ_{ij}. In each component Ω_i, the weak formulation of the second–order differential equation (1) can be obtained by multiplying it with the virtual energy density $\bar{e}_i$, and by integrating the equation over the component's domain. After integration by parts, the following is obtained:

$$\iint_{\Omega_i} (\frac{c_{gi}^2}{\eta_i\omega}\nabla\bar{e}_i \cdot \nabla e_i + \eta_i\omega\bar{e}_i e_i)\,d\Omega$$
$$= \iint_{\Omega_i}\bar{e}_i\pi_i\,d\Omega - \int_{\Gamma_i^e\cup\Gamma_i^q\cup\Gamma_{ij}}\bar{e}_i(\mathbf{n}_i\cdot\mathbf{I}_i)\,d\Gamma, \quad i=1,2 \tag{2}$$

where $\nabla e_i = [\partial e_i/\partial x, \partial e_i/\partial y]^T$ is the gradient vector of the energy density; $\mathbf{n}_i$ is the unit outward normal vector to the boundary; and $\mathbf{I}_i$ is the time– and space–averaged energy intensity. Since the last integral on the right side of (2) represents the power flow on the boundary, the following relation can be defined:

$$q_i = \mathbf{n}_i \cdot \mathbf{I}_i \tag{3}$$

By using the fact that the virtual energy density $\bar{e}_i$ vanishes on the boundary Γ_i^e, and that the power flow on the boundary Γ_i^q is given, the variational equation of the built–up structure in Figure 1 can be written as

American Institute of Aeronautics and Astronautics

$$\sum_{i=1}^{2} \iint_{\Omega_i} \left(\frac{c_{gi}^2}{\eta_i \omega} \nabla \overline{e}_i \cdot \nabla e_i + \eta_i \omega \overline{e}_i e_i \right) d\Omega \tag{4}$$

$$= \sum_{i=1}^{2} \left(\iint_{\Omega_i} \overline{e}_i \pi_i \, d\Omega - \int_{\Gamma_i^q} \overline{e}_i \hat{q}_i \, d\Gamma \right) - \int_{\Gamma_{12}} (\overline{e}_1 q_1 + \overline{e}_2 q_2) \, d\Gamma$$

with the interface condition $q_1 + q_2 = 0$ on Γ_{12}, and for all $\overline{e}_i$ that satisfy the above-mentioned boundary conditions.

In a general setting, let $\mathbf{e}$ denote a composite vector of energy density fields in the components making up the built–up structure; that is, $\mathbf{e} = [e_1, e_2, \ldots, e_r]^T$, where $e_i \in [H^0(\Omega_i)]^2$ represents the energy density of the component Ω_i. The space of kinematically admissible fields is defined as a set of energy densities that satisfy homogeneous boundary and interface conditions between components. That is,

$$Z = \{\mathbf{e} \in W : \mathbf{e} = 0 \text{ on } \Gamma^e \text{ and } q_i + q_i = 0 \text{ on } \Gamma_{ij}\} \tag{5}$$

where the product space $W = \Pi_{i=1}^{r}[H^0(\Omega_i)]^2$ is the space of energy density fields that satisfy the required degree of smoothness, $\Gamma^e = \Gamma_1^e \cup \Gamma_2^e \cup \cdots \cup \Gamma_r^e$ is the essential boundary where the energy density function is prescribed, and Γ_{ij} is the common boundary of components i and j. By using this definition, (4) satisfies for every $\overline{\mathbf{e}} \equiv [\overline{e}_1, \overline{e}_2, \ldots, \overline{e}_r]^T$ belonging to the space Z of kinematically admissible fields.

For derivational convenience, variational equation (4) can be rewritten using bilinear and linear forms as

$$a_\Omega(\mathbf{e}, \overline{\mathbf{e}}) + b_\Gamma(\mathbf{e}, \overline{\mathbf{e}}) = \ell_\Omega(\overline{\mathbf{e}}), \qquad \forall \overline{\mathbf{e}} \in Z \tag{6}$$

where bilinear and linear forms are defined as

$$a_\Omega(\mathbf{e}, \overline{\mathbf{e}}) \equiv \sum_{i=1}^{r} \iint_{\Omega_i} \left(\frac{c_{gi}^2}{\eta_i \omega} \nabla \overline{e}_i \cdot \nabla e_i + \eta_i \omega \overline{e}_i e_i \right) d\Omega \tag{7}$$

$$\ell_\Omega(\overline{\mathbf{e}}) \equiv \sum_{i=1}^{r} \left[\iint_{\Omega_i} \overline{e}_i \pi_i \, d\Omega - \int_{\Gamma_i^q} \overline{e}_i \hat{q}_i \, d\Gamma \right] \tag{8}$$

$$b_\Gamma(\mathbf{e}, \overline{\mathbf{e}}) \equiv \sum_{(i,j)=1}^{N_r} \int_{\Gamma_{ij}} (\overline{e}_i q_i + \overline{e}_i q_j) \, d\Gamma \tag{9}$$

where N_r is the number of interfaces within the built–up structure. Note that the bilinear form $a_\Omega(\cdot, \cdot)$ is symmetric with respect to its arguments, while $b_\Gamma(\cdot, \cdot)$ is not. In fact, with its interface condition, $b_\Gamma(\cdot, \cdot)$ represents the conservation of power flow across the discontinuity of material property or junction geometry.

From a design point of view, the parameters that appear in (6) can serve as design variables. In the case of a plate–bending problem, for example, the group speed can be written as

$$c_g = 2\sqrt[4]{\frac{\omega^2 D}{\rho h}} = 2\sqrt[4]{\frac{\omega^2 E h^2}{12 \rho (1 - v^2)}} \tag{10}$$

where ρ is the density of the plate, E is Young's modulus, v is the Poisson's ratio, h is the thickness of the plate, and D is the flexural rigidity. As will be shown in Section 3, the parameters in (10), as well as the hysteresis–damping factor η will serve as design variables.

The analytical solution to structural–acoustic equation (6) can only be obtained for a simple geometry. In general structures, FEM is often used to approximate the solution to (6). The FEM process involves dividing the structural component's domain Ω_i into a set of simple finite elements $\Omega_i^m (m = 1, \ldots, N_i)$, and then imposing equation (6) on each element. The global system of matrix equations can be obtained through the assembly process. However, the EFA assembly process is different from conventional FEM because energy density is not continuous across structural junctions.[14] Instead of state variable continuity, the power flow conservation is used in the assembly process. The structural junction appears when either the material property or the geometric configuration changes. If no junction exists, then a regular finite element assembly process can be used.

In FEM, the energy density in finite element Ω_i^m is approximated using an interpolation vector $\{\mathbf{N}_i^m\}$ and a nodal energy density vector $\{\mathbf{E}_i^m\}$ as

$$e_i^m = \{\mathbf{N}_i^m\}^T \{\mathbf{E}_i^m\} \tag{11}$$

The dimensions $\{\mathbf{N}_i^m\}$ and $\{\mathbf{E}_i^m\}$ are the same as the number of nodes in element Ω_i^m. Then, the nodal energy density vector of component Ω_i is defined by

$$\{\mathbf{E}_i\} = \{\mathbf{E}_i^1, \mathbf{E}_i^2, \ldots, \mathbf{E}_i^{N_i}\}^T \tag{12}$$

The same interpolation method will be used for the virtual energy density $\overline{e}_i$ in Galerkin approximation. By using the standard Gauss integration method, the bilinear and linear forms in equations (7) – (9) are approximated by

$$\sum_{i=1}^{r} \iint_{\Omega_i} \left(\frac{c_{gi}^2}{\eta_i \omega} \nabla \overline{e}_i \cdot \nabla e_i + \eta_i \omega \overline{e}_i e_i \right) d\Omega$$
$$\approx \sum_{i=1}^{r} \{\overline{\mathbf{E}}_i\}^T [\mathbf{K}_i] \{\mathbf{E}_i\} \tag{13}$$

$$\sum_{i=1}^{r} \left[\iint_{\Omega_i} \overline{e}_i \pi_i \, d\Omega - \int_{\Gamma_i^q} \overline{e}_i \hat{q}_i \, d\Gamma \right] \approx \sum_{i=1}^{r} \{\overline{\mathbf{E}}_i\}^T \{\mathbf{F}\} \tag{14}$$

$$\sum_{(i,j)=1}^{N_r} \int_{\Gamma_{ij}} (\overline{e}_i q_i + \overline{e}_j q_j) \, d\Gamma \approx \sum_{(i,j)=1}^{N_r} \{\overline{\mathbf{E}}_i, \overline{\mathbf{E}}_j\} \begin{Bmatrix} \mathbf{Q}_i \\ \mathbf{Q}_j \end{Bmatrix} \tag{15}$$

The global system of matrix equations can be obtained through the assembly process. After imposing the essential boundary condition, the global system of matrix equations is obtained as

$$[\mathbf{K}]\{\mathbf{E}\} = \{\mathbf{F}\} - \{\mathbf{Q}\} \tag{16}$$

where $\{\mathbf{E}\} = \{E_1, E_2, \ldots, E_r\}^T$, $\{\mathbf{F}\} = \{F_1, F_2, \ldots, F_r\}^T$, $\{\mathbf{Q}\} = \{Q_1, Q_2, \ldots, Q_r\}^T$, and

$$[\mathbf{K}] = \overset{r}{\underset{i=1}{\mathbf{A}}}([\mathbf{K}_i]) \qquad (17)$$

where **A** denotes the assembly operator that maps the component's coefficient matrix into the global coefficient matrix.

When discontinuities exist in the material property and junction shape, the power flow vector $\{\mathbf{Q}_i\}$ must be calculated from the conservation of power flow across the junction. This process is equivalent to the construction of kinematically admissible fields, defined in (5). For simplicity, let the components Ω_i and Ω_j have a single element i and j, respectively, and let elements i and j share the discontinuous junction. Then, the conservation requirement yields the following relation between the power flow and energy density of two adjacent elements:

$$\begin{Bmatrix} \mathbf{Q}_i \\ \mathbf{Q}_j \end{Bmatrix} = [\mathbf{J}_{ij}] \begin{Bmatrix} \mathbf{E}_i \\ \mathbf{E}_j \end{Bmatrix} \qquad (18)$$

Note that it is necessary to define duplicate nodes along the junction. Construction of the junction matrix $[\mathbf{J}_{ij}]$ involves calculating the power transfer coefficient.[14] Thus, it is critical to calculate the power transfer coefficient in the assembly process. In addition, this coefficient is a function of the material property, panel thickness, and junction geometry, which are design variables.

Given the relation in (18), the power flow vector in (16) moves to the left side of the matrix equation. Thus, the assembled matrix of elements i and j becomes

$$\left[\begin{bmatrix} \mathbf{K}_i & \mathbf{0} \\ \mathbf{0} & \mathbf{K}_j \end{bmatrix} + [\mathbf{J}_{ij}] \right] \begin{Bmatrix} \mathbf{E}_i \\ \mathbf{E}_j \end{Bmatrix} = \begin{Bmatrix} \mathbf{F}_i \\ \mathbf{F}_j \end{Bmatrix} \qquad (19)$$

Due to the asymmetry of the junction matrix $[\mathbf{J}_{ij}]$, the coefficient matrix in (19) is not symmetric. However, it will be shown in the development of the design sensitivity formulation that such asymmetry does not cause any further computational cost in solving the adjoint problem.

Langley and Heron[17] presented an analytical method for calculating the power transfer coefficient for arbitrary angled plate–to–plate junctions. The same method is used in this paper for energy flow and design sensitivity analysis. The analytical method for calculating power transfer coefficients uses a junction composed of semi-infinite plates. The rationale for applying this semi-infinite theory to the finite-dimension has been discussed by Cremer et al.[18] through the frequency–averaging process at high frequencies.

From (15), the power flow vector $\{\mathbf{Q}_i\}$ is obtained by integrating the local power flow q_i along the junction Γ_{12} as

$$\begin{Bmatrix} \mathbf{Q}_1 \\ \mathbf{Q}_2 \end{Bmatrix} = \begin{Bmatrix} \int_{\Gamma_{12}} \{\mathbf{N}_1\} q_1 \, d\Gamma \\ \int_{\Gamma_{12}} \{\mathbf{N}_2\} q_2 \, d\Gamma \end{Bmatrix} \equiv [\mathbf{J}_{12}] \begin{Bmatrix} \mathbf{E}_1 \\ \mathbf{E}_2 \end{Bmatrix} \qquad (20)$$

where $\{\mathbf{E}_i\}$ is the $N_p \times 1$ nodal energy density vector of element i, and $[\mathbf{J}_{12}]$ is the $2N_p \times 2N_p$ junction matrix. This relation is assembled in the global matrix equation using the local–to–global Boolean operation. Since the interpolation function of those nodes that do not belong to the junction boundary vanishes on Γ_{12}, the size of the junction matrix can be further reduced if such a situation is taken into account.

The junction relation in (20) corresponds to the simplest situation in the plate–to–plate connection. If two members join with an arbitrary angle, then the bending, longitudinal, and shear waves must be considered simultaneously. In such a case, the size of the junction matrix becomes $6N_p \times 6N_p$. The junction matrix becomes more complicated when multiple components are connected at the junction. However, the same conservation of power flow can be used, although with algebraic complications.

3. DESIGN SENSITIVITY ANALYSIS

Design sensitivity is the gradient of a performance measure with respect to design variables. In the structural–acoustic problem, vibration energy often serves as a performance measure. This study focuses on parameter sensitivity analysis in which the parameter of a structural–acoustic problem is a design variable. The thickness of the plate, the material property, the power transfer coefficient, and the hysteresis–damping factor are all examples of parametric design variables.

Throughout this paper, u denotes a parametric design variable. Let ψ be a function that depends on current design u, and assume that $\psi(u)$ is continuous with respect to design u. If the current design is perturbed in the direction of δu (arbitrary), and ε is a scalar parameter that controls perturbation size, then the variation of $\psi(u)$ in the direction of δu is defined as

$$\psi'_{\delta u} \equiv \frac{d}{d\varepsilon} \psi(u + \varepsilon \delta u) \Big|_{\varepsilon=0} = \frac{\partial \psi}{\partial u} \delta u \qquad (21)$$

Throughout this paper, the prime symbol " ′ " is the first variation in the calculus of variations.[19] For convenience, subscribed δu will often be ignored. The term "derivative" or "differentiation" will often be used to denote the variation in (21), because the coefficient of δu (i.e., $\partial \psi / \partial u$) will be calculated in practice. If the variation of a function is continuous and linear with respect to δu, then the function is differentiable (more precisely, it is Fréchet differentiable).

Without mathematical proof, the solution **e** to the energy flow equation in Section 2, given here in the rewritten form

$$a_u(\mathbf{e}, \overline{\mathbf{e}}) + b_u(\mathbf{e}, \overline{\mathbf{e}}) = \ell_u(\overline{\mathbf{e}}), \qquad \forall \overline{\mathbf{e}} \in Z \qquad (22)$$

is differentiable with respect to the design. That is, the variation

$$\mathbf{e}' = \mathbf{e}'(\mathbf{x}; u, \delta u) \equiv \frac{d}{d\varepsilon} \mathbf{e}(\mathbf{x}; u + \varepsilon \delta u)\bigg|_{\varepsilon=0} \qquad (23)$$

exists, and is the first variation of the solution to (22) at design u and in direction δu of the design change. Note that $\mathbf{e}'$ is a function of independent variable $\mathbf{x}$, and depends on design u and direction δu. In (22), the subscribed u is used to emphasize that bilinear and linear forms depend on design u.

In addition, each of the bilinear and linear forms encountered in Section 2 is assumed to be differentiable with respect to the design. That is,

$$a'_{\delta u}(\mathbf{e}, \overline{\mathbf{e}}) \equiv \frac{d}{d\varepsilon} a_{u+\varepsilon\delta u}(\tilde{\mathbf{e}}, \overline{\mathbf{e}})\bigg|_{\varepsilon=0} \qquad (24)$$

$$\ell'_{\delta u}(\overline{\mathbf{e}}) \equiv \frac{d}{d\varepsilon} \ell_{u+\varepsilon\delta u}(\overline{\mathbf{e}})\bigg|_{\varepsilon=0} \qquad (25)$$

$$b'_{\delta u}(\mathbf{e}, \overline{\mathbf{e}}) \equiv \frac{d}{d\varepsilon} b_{u+\varepsilon\delta u}(\tilde{\mathbf{e}}, \overline{\mathbf{e}})\bigg|_{\varepsilon=0} \qquad (26)$$

exist, where $\tilde{\mathbf{e}}$ denotes the state variable $\mathbf{e}$, with the dependence on ε being suppressed, and $\overline{\mathbf{e}}$ is independent of ε. For example, $a'_{\delta u}(\mathbf{e}, \overline{\mathbf{e}})$ is the first variation of the bilinear form a_u in the direction of δu. It is assumed that this first variation is continuous and linear in δu; hence, it is the Fréchet derivative of a_u with respect to the design, and as evaluated in the direction of δu. In fact, Equations (24) – (26) are the contributions from the bilinear and linear forms that are explicitly dependent on the design.

3.1 Direct Differentiation Method

A direct differentiation method calculates the variation of the energy density in (23) by differentiating structural–acoustic equation (22) as

$$a_u(\mathbf{e}', \overline{\mathbf{e}}) + b_u(\mathbf{e}', \overline{\mathbf{e}}) = \ell'_{\delta u}(\overline{\mathbf{e}}) - a'_{\delta u}(\mathbf{e}, \overline{\mathbf{e}}) - b'_{\delta u}(\mathbf{e}, \overline{\mathbf{e}}), \\ \forall \overline{\mathbf{e}} \in Z \qquad (27)$$

The left side of (27) presents the terms that are implicitly dependent on the design. Thus, design sensitivity equation (27) solves the implicitly dependent terms by using the explicitly dependent ones. The left side of (27) is the same as that of (22) if $\mathbf{e}'$ is replaced by $\mathbf{e}$. Thus, the design sensitivity equation uses the same coefficient matrix from structural–acoustic analysis with a different load on the right side.

Next, consider a structural–acoustic performance measure that can be written in integral form, as

$$\psi = \iint_\Omega g(\mathbf{e}, \nabla \mathbf{e}, u + \varepsilon \delta u) \, d\Omega \qquad (28)$$

where function g is continuously differentiable with respect to its arguments. Functionals in the form of (28) represent a wide variety of structural–acoustic performance measures. For example, the volume of a structural component can be written with a g that depends explicitly on u; energy intensity can be written in terms of u and $\nabla \mathbf{e}$; and energy density at a point can be formally written using the Dirac–δ measure.

To develop the design sensitivity formula, take the variation of the functional in (28), as

$$\psi' = \iint_\Omega (g_{,\mathbf{e}} \cdot \mathbf{e}' + g_{,\nabla \mathbf{e}} \cdot \nabla \mathbf{e}' + g_{,u} \delta u) \, d\Omega \qquad (29)$$

From the definition of function g, it is assumed that the expressions of $g_{,\mathbf{e}}$, $g_{,\nabla\mathbf{e}}$, and $g_{,u}$ are available. Thus, from the solution $\mathbf{e}'$ of design sensitivity equation (27), the variation ψ' can readily be evaluated in the direct differentiation method.

3.2 Adjoint Variable Method

Recall that $\mathbf{e}'$ and $\nabla \mathbf{e}'$ depend on the design change direction δu. The objective of the adjoint variable method is to obtain an explicit expression of ψ' in terms of δu, which requires rewriting the first two terms on the right of (29) explicitly in terms of δu. An adjoint equation is introduced for that purpose by replacing $\mathbf{e}'$ in (29) with a virtual energy density $\overline{\boldsymbol{\lambda}} = \{\overline{\lambda}_1, \overline{\lambda}_2, \dots, \overline{\lambda}_r\}^T$, and by equating the terms involving $\overline{\boldsymbol{\lambda}}$ in (29) to the bilinear forms in (22), yielding the adjoint equation for adjoint variable $\boldsymbol{\lambda}$:

$$a_u(\overline{\boldsymbol{\lambda}}, \boldsymbol{\lambda}) + b_u(\overline{\boldsymbol{\lambda}}, \boldsymbol{\lambda}) = \iint_\Omega (g_{,\mathbf{e}} \cdot \overline{\boldsymbol{\lambda}} + g_{,\nabla\mathbf{e}} \cdot \nabla\overline{\boldsymbol{\lambda}}) \, d\Omega, \\ \forall \overline{\boldsymbol{\lambda}} \in Z \qquad (30)$$

where the solution $\boldsymbol{\lambda} = \{\lambda_1, \lambda_2, \dots, \lambda_r\}^T$ is desired, which is the adjoint energy density associated with the performance measure in (28).

The intention is to express the first two terms on the right of (29) in terms of adjoint variable $\boldsymbol{\lambda}$. Since (30) satisfies for all $\overline{\boldsymbol{\lambda}} \in Z$, and since $\mathbf{e}'$ belongs to space Z, equation (30) may be evaluated at a specific $\overline{\boldsymbol{\lambda}} = \mathbf{e}'$. After substitution, the following is obtained:

$$a_u(\mathbf{e}', \boldsymbol{\lambda}) + b_u(\mathbf{e}', \boldsymbol{\lambda}) = \iint_\Omega (g_{,\mathbf{e}} \cdot \mathbf{e}' + g_{,\nabla\mathbf{e}} \cdot \nabla\mathbf{e}') \, d\Omega \qquad (31)$$

where the right side is the same as the first two terms of the right side of (29), which it is now desirable to write explicitly in terms of δu. Similarly, design sensitivity equation (27) may be evaluated at a specific $\overline{\mathbf{e}} = \boldsymbol{\lambda}$ to obtain

$$a_u(\mathbf{e}', \boldsymbol{\lambda}) + b_u(\mathbf{e}', \boldsymbol{\lambda}) = \ell'_{\delta u}(\boldsymbol{\lambda}) - a'_{\delta u}(\mathbf{e}, \boldsymbol{\lambda}) - b'_{\delta u}(\mathbf{e}, \boldsymbol{\lambda}) \qquad (32)$$

The left sides of (31) and (32) are equal, yielding the following desired relation:

$$\iint_\Omega (g_{,\mathbf{e}} \cdot \mathbf{e}' + g_{,\nabla\mathbf{e}} \cdot \nabla\mathbf{e}') \, d\Omega \\ = \ell'_{\delta u}(\boldsymbol{\lambda}) - a'_{\delta u}(\mathbf{e}, \boldsymbol{\lambda}) - b'_{\delta u}(\mathbf{e}, \boldsymbol{\lambda}) \qquad (33)$$

where the right side is linear in δu and can be evaluated

once the state variable **e** and the adjoint variable **λ** are determined to be the solutions to (22) and (30), respectively. Substituting the result of (33) into (29), the explicit design sensitivity of ψ is obtained as

$$\psi' = \ell'_{\delta u}(\boldsymbol{\lambda}) - a'_{\delta u}(\mathbf{e},\boldsymbol{\lambda}) - b'_{\delta u}(\mathbf{e},\boldsymbol{\lambda}) + \iint_\Omega g_{,u}\delta u \, d\Omega \qquad (34)$$

where the first three terms on the right depend on the specific problem under investigation.

As was shown in (27), the direct differentiation method uses the same coefficient matrix as response analysis. However, the format of adjoint equation (30) is different from response analysis because $b_u(\mathbf{e},\bar{\mathbf{e}})$ is not symmetric with respect to its arguments. In the early development of the adjoint variable method,[20] the symmetric property of the bilinear form plays an important role. However, the definition of the adjoint problem in (30) does not require the symmetric property of the bilinear form.

3.3 Analytical Example

In this section, explicit expressions of variations in (24)–(26) are developed for the plate component, since this component is commonly used in engineering applications. For notational simplicity, expressions in this section correspond to a single component without including the component's index. When a constant input power and a constant power flow are supplied to the structure (see Figure 2), π and $\hat{q}$ are independent of the parametric design variable, i.e., $\pi' = \hat{q}' = 0$. Thus, from its definition in (8), the variation of $\ell_u(\bar{e})$ vanishes, i.e., $\ell'_{\delta u}(\bar{e}) = 0$. Since the bilinear form $b_u(e,\bar{e})$ is calculated from the conservation of power flow across a junction, its variation will be calculated in the next section, along with finite element discretization.
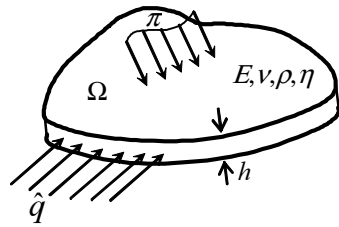

Figure 2 Design Variables of a Plate Component

The variation of bilinear form $a_u(e,\bar{e})$ depends on the parametric design variable. For derivational convenience, the hysteresis–damping factor is treated separately from other design variables. According to the definition of the variation in (24), the bilinear form in (7) is differentiated with respect to η to obtain

$$a'_{\delta\eta}(e,\bar{e}) = \iint_\Omega (-\frac{c_g^2}{\eta^2\omega}\nabla\bar{e}\cdot\nabla e + \omega\bar{e}\,e)\delta\eta \, d\Omega \qquad (35)$$

For other types of parametric design variables, the dependence of $a_u(e,\bar{e})$ on the design is only through the group speed c_g. Thus, the variation of $a_u(e,\bar{e})$ is obtained by

$$a'_{\delta u}(e,\bar{e}) = \iint_\Omega (\frac{2c_g}{\eta\omega}\nabla\bar{e}\cdot\nabla e)\delta c_g \, d\Omega \qquad (36)$$

where δc_g is the variation of the group speed. In the case of a bending–to–bending vibration, the expression of δc_g can be obtained from its definition in (10), which is summarized in Table 1.

Since results from the structural–acoustic problem are already available, the variation $a'_{\delta u}(e,\bar{e})$ can be readily evaluated for a given δu. In the case of the adjoint variable method, $a'_{\delta u}(e,\lambda)$ is evaluated with the adjoint result λ.

Table 1 Variation of the Group Speed

Design Variable	δc_g
H	$(c_g/2h)\delta h$
E	$(c_g/4E)\delta E$
v	$[vc_g/2(1-v^2)]\delta v$
ρ	$-(c_g/4\rho)\delta\rho$

3.4 Finite Element Approximation

In order to be consistent and efficient, discretization of the design sensitivity equation must follow the same approximation method as the energy flow analysis described in Section 2. In this section, finite element approximation of the design sensitivity equation is presented using direct differentiation and adjoint variable methods.

Discretization of the structural fictitious load in (24) can be obtained using the energy density **e**. In a plate component, for example, $a'_{\delta u}(\mathbf{e},\bar{\mathbf{e}})$ in (36) can be approximated by

$$a'_{\delta u}(\mathbf{e},\bar{\mathbf{e}}) = \sum_{i=1}^{2} \iint_{\Omega_i} (\frac{2c_{gi}}{\eta_i\omega}\nabla\bar{e}_i\cdot\nabla e_i)\delta c_{gi}d\Omega$$
$$\approx \{\bar{\mathbf{E}}_1 \quad \bar{\mathbf{E}}_2\}\begin{Bmatrix} \mathbf{F}_1^a \\ \mathbf{F}_2^a \end{Bmatrix}\delta u \qquad (37)$$

where $\mathbf{F}_i^a$ is the nodal fictitious load vector of component i, and δu is the variation of design that appears in Table 1.

Although $a'_{\delta u}(\mathbf{e},\bar{\mathbf{e}})$ in (36) is calculated in the continuum domain followed by finite element approximation, it is convenient to calculate $b'_{\delta u}(\mathbf{e},\bar{\mathbf{e}})$ by differentiating the discrete vector in (15) and (18), which corre-

sponds to differentiating the junction matrix. Thus, we obtain

$$b'_{\delta u}(\mathbf{e}, \overline{\mathbf{e}}) \approx \{\overline{\mathbf{E}}_1 \quad \overline{\mathbf{E}}_2\}[\mathbf{J}'_{12}]\begin{Bmatrix} \mathbf{E}_1 \\ \mathbf{E}_2 \end{Bmatrix} \qquad (38)$$

Since the left side of sensitivity equation (27) is the same as the left side of (22), by replacing $\mathbf{e}'$ with $\mathbf{e}$ the approximated sensitivity equation has the same coefficient matrix as in (19). The global sensitivity matrix equation is obtained from (27), (38), and (37), as

$$\left[\begin{bmatrix} \mathbf{K}_1 & \mathbf{0} \\ \mathbf{0} & \mathbf{K}_2 \end{bmatrix} + [\mathbf{J}_{12}]\right]\begin{Bmatrix} \mathbf{E}'_1 \\ \mathbf{E}'_2 \end{Bmatrix} = -\begin{Bmatrix} \mathbf{F}_1^a \\ \mathbf{F}_2^a \end{Bmatrix}\delta u - [\mathbf{J}'_{12}]\begin{Bmatrix} \mathbf{E}_1 \\ \mathbf{E}_2 \end{Bmatrix} \quad (39)$$

where the nodal energy density variation $\{\mathbf{E}'_i\}$ is solved. After computing $\{\mathbf{E}'\} = \{\mathbf{E}'_1 \quad \mathbf{E}'_2\}^T$, the variation of energy density is calculated using the same approximation method used in (11); that is,

$$e'_i = \{\mathbf{N}_i\}^T \{\mathbf{E}'_i\} \qquad (40)$$

and the sensitivity of the performance measure in (29) is calculated using the chain rule of differentiation and numerical integration. Since the coefficient matrix of (39) is factorized during energy flow analysis, (39) can be solved very efficiently.

With the adjoint variable method, adjoint variable λ is approximated using the same shape function as the energy density function; i.e., $\lambda_i = \{\mathbf{N}_i\}^T \{\mathbf{\Lambda}_i\}$. The adjoint load, defined in (30), is calculated using the same finite element approximation and numerical integration method, as

$$\iint_\Omega (g_{,e} \cdot \overline{\lambda} + g_{,\nabla e} \cdot \nabla \overline{\lambda}) \, d\Omega \approx \{\overline{\mathbf{\Lambda}}_1 \quad \overline{\mathbf{\Lambda}}_2\}^T \begin{Bmatrix} \mathbf{F}_1^{adj} \\ \mathbf{F}_2^{adj} \end{Bmatrix} \qquad (41)$$

where $\{\overline{\mathbf{\Lambda}}_1 \quad \overline{\mathbf{\Lambda}}_2\}^T$ is the virtual nodal adjoint variable. In the above equation, the adjoint load is independent of design variables; it only depends on the performance measure. The left side of adjoint equation (30) is the transpose of state equation (22) because the bilinear form $b_u(\cdot, \cdot)$ is not symmetric. Thus, the adjoint problem is defined using the transpose of the coefficient matrix in (19), as

$$\left[\begin{bmatrix} \mathbf{K}_1 & \mathbf{0} \\ \mathbf{0} & \mathbf{K}_2 \end{bmatrix} + [\mathbf{J}_{12}]\right]^T \begin{Bmatrix} \mathbf{\Lambda}_1 \\ \mathbf{\Lambda}_2 \end{Bmatrix} = \begin{Bmatrix} \mathbf{F}_1^{adj} \\ \mathbf{F}_2^{adj} \end{Bmatrix} \qquad (42)$$

Even if the coefficient matrix in (42) is the transpose of the coefficient matrix in (19), the latter can still be used to solve the former. Thus, the computational costs of solving adjoint equation (39) and sensitivity equation (42) are the same.

After solving the adjoint variable $\{\lambda\}$, the performance sensitivity in (34) is obtained using the numerical integration rule, as

$$\psi' = \iint_\Omega g_{,u} \delta u \, d\Omega - \{\mathbf{\Lambda}_1 \quad \mathbf{\Lambda}_2\}\begin{Bmatrix} \mathbf{F}_1^a \\ \mathbf{F}_2^a \end{Bmatrix}\delta u$$

$$\qquad\qquad (43)$$

$$-\{\mathbf{\Lambda}_1 \quad \mathbf{\Lambda}_2\}[\mathbf{J}'_{12}]\begin{Bmatrix} \mathbf{E}_1 \\ \mathbf{E}_2 \end{Bmatrix}$$

As shown in the above equation, the adjoint variable method still requires calculation of the fictitious load $\{\mathbf{F}^a\}$ and $[\mathbf{J}'_{12}]$, which appear in the direct differentiation method. Thus, both methods have the same computational costs, except for the number of matrix equations that need to be solved. The direct differentiation method solves the system of matrix equations according to the number of design variables, while the adjoint variable method solves it according to the number of performance measures.

4. NUMERICAL EXAMPLES

4.1 Parameter Study

In order to control power flow between structural members, it is necessary to control the power transfer coefficient. Since this coefficient is the ratio between incident and transmitted powers, a panel thickness change will affect it. Figure 3 shows two co-planar plates with the same material properties ($E = 209$ GPa, $v = 0.3$, $\rho = 7,800$ kg/m^3). An incident wave with a frequency of $\omega = 2.0$ kHz is considered. The thickness of Plate 1 changes from 0.5 mm to 1.5 mm, while the thickness of Plate 2 is fixed at 1.0 mm. Only bending–to–bending power transmission is considered, because the plates are co-planar. As the thickness begins to differ between the two plates, the values of the power transfer coefficients change from one. The maximum change occurs when the thickness of Plate 1 is 0.5 mm, and the value of τ_{12}^{BB} is reduced to 70%.
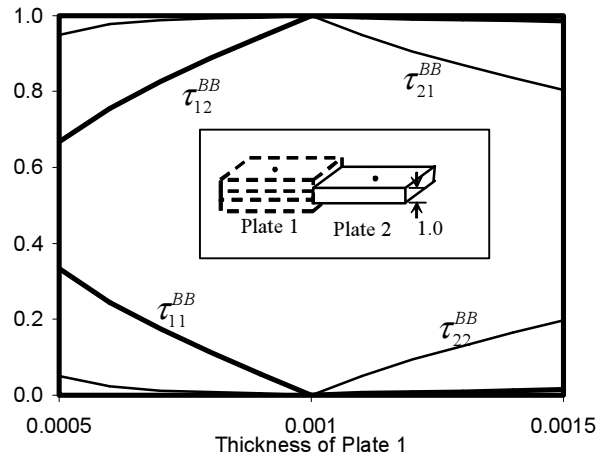

Figure 3 Variations of the Power Transfer Coefficients as a Function of Panel Thickness

To investigate further the effect of structural design variables on the power transfer coefficient, variations of energy density as a function of panel thickness are studied for the co-planar plates, as shown in Figure 4. Unit power density (J/m^2·s) is applied at the center of Plate 1. In Figure 3, Point 1 corresponds to the center of Plate 1, while Point 2 corresponds to the center of Plate 2. A hysteresis–damping factor of $\eta = 0.01$ is used for both plates. The plates have the same initial thickness of 1.0 mm. The energy densities at the center point of these plates are plotted by changing the thickness of the left plate from 0.5 mm to 1.5 mm. By reducing the thickness of the left plate by 0.5 mm, its energy density increases by 30% at the center, while the energy density decreases by 64% at the center of the right plate. Consequently, in this simple example the ratio of the energy density change appears to be greater than the ratio of the design variable change.

Although the differentiability of energy density with respect to the design is not proved in the theoretical sections of this study, the power transfer coefficient in Figure 3 and the energy density in Figure 4 show smooth variations of the energy density as a function of the thickness design variable.
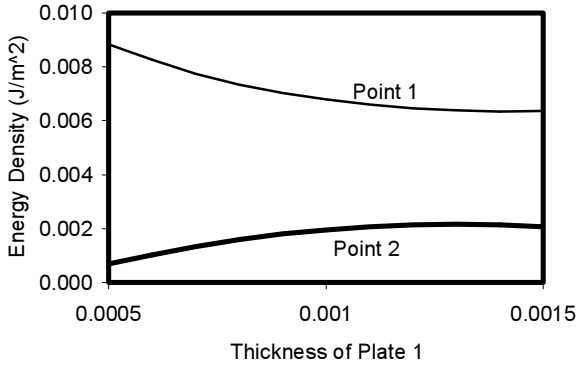

Figure 4 Variations of the Energy Densities as a Function of a Panel Thickness

4.2 Power Transfer Coefficient Sensitivity

The parametric study in Section 4.1 illustrates that the power transfer coefficients depend on design variables. For example, Figure 5 plots the variations of a bending–to–bending power transfer coefficient as a function of thickness design variables. Two semi-infinite plates are connected at a right angle. The thickness of Plate 1 (incident plate) is fixed at 1.0 mm, while the thickness of Plate 2 varies from 0.5 mm to 1.5 mm. The same material properties ($E = 209$ GPa, $v = 0.3$, $\rho = 7,800$ kg/m^3) are used for both plates. An incident wave with a frequency of $\omega = 20$ kHz is considered. In contrast to the co-planar plates in Figure 3, the reflection power transfer coefficient τ_{11}^{BB} is greater than the trans-

ferred power transfer coefficient τ_{12}^{BB}. In addition, the summation of τ_{11}^{BB} and τ_{12}^{BB} does not equal one because the bending incident wave is transmitted as bending, in-plane, and shear wave, although the bending–to–bending transmission is the dominant mode. The sensitivity of these power transfer coefficients with respect to plate thickness is represented by the slope of curves in Figure 5.

The analytical sensitivity of the power transfer coefficient is found by differentiating the procedure for calculating the power transfer coefficient. In order to verify the accuracy, Figure 6 compares analytical sensitivity results of the power transfer coefficients with sensitivity results calculated using the finite difference method (FDM). The finite difference sensitivity of τ_{11}^{BB}, for example, can be calculated from the following formula:

$$\tau_{11}^{BB\prime}(h) \approx \frac{\tau_{11}^{BB}(h+\Delta h) - \tau_{11}^{BB}(h)}{\Delta h} \qquad (44)$$

where $\Delta h = 0.01$ mm is used. In general, sensitivity $\tau_{11}^{BB\prime}$ from Eq. (44) is more accurate as perturbation size Δh decreases. However, numerical noise becomes dominant if Δh is so small that the change in τ_{11}^{BB} is smaller than the machine's significant digit. Thus, it is always difficult to select the appropriate perturbation size in FDM. In Figure 6, "$\tau_{11}^{BB\prime}$ FDM" represents the sensitivity of τ_{11}^{BB} calculated using the finite difference method, while "$\tau_{11}^{BB\prime}$ Analytical" represents the sensitivity of τ_{11}^{BB} calculated from the proposed continuum sensitivity formula. As shown in Figure 6, analytical sensitivity results agree with finite difference sensitivity results.
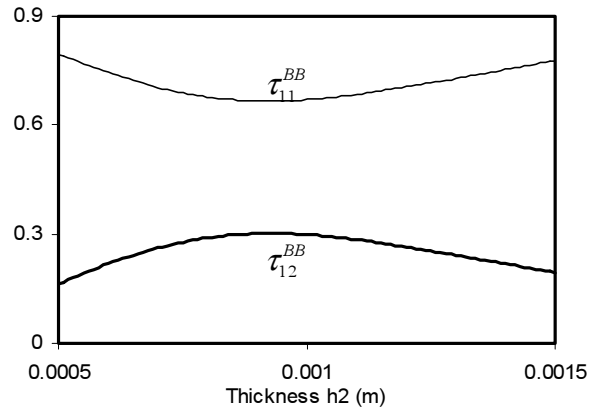

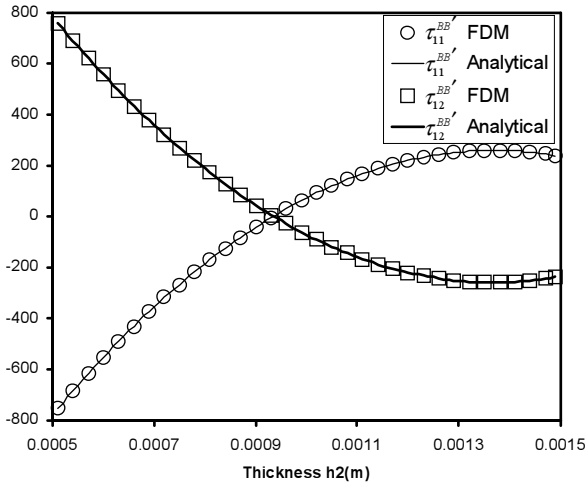Figure 5 Variation of the Power Transfer Coefficient as a Function of the Plate Thickness Design ($\omega = 2.0$ kHz)

American Institute of Aeronautics and Astronautics

Figure 6 Sensitivity Results of Power Transfer Coefficients Compared with the Finite Difference Results for the Plate Thickness Design (ω = 2.0 kHz)

4.3 Energy Density Sensitivity

Power transfer coefficient sensitivity results in Section 4.2 can be obtained from the analytical expression. However, the sensitivity of the energy density can only be calculated by solving the sensitivity equation for the direct differentiation method, or by solving the adjoint equation for the adjoint variable method. In this section, the accuracy of energy density sensitivity is compared with sensitivity results obtained from FDM.

Consider two plates from Section 4.2 that form a right angle to each other. In addition to having the same thickness and material properties as in Section 4.2, these plates also have a hysteresis–damping factor of η = 0.01. The dimension of each plate is 1 m × 1 m × 0.001 m, and 100 finite elements are used to approximate each plate. Figure 7 shows the plate geometry with 200 finite elements. A unit power density with frequency 2.0 kHz is applied at node 61, which is the center of Plate 1. The objective is to estimate the variation of energy density as a function of Plate 1's thickness using the sensitivity calculation method.

Figure 8 plots the sensitivity of energy density functions with respect to the thickness design of Plate 1. The location of point P1 is at the center of Plate 1, while P2 is at the center of Plate 2. "DSA P1" is the design sensitivity of energy density at P1 calculated using the proposed method, while "FDM P1" is the design sensitivity calculated using the finite difference method. A direct differentiation method is used to calculate the sensitivity of energy density functions. As the thickness of Plate 1 increases, more power is transferred to Plate 2. Thus, the energy density sensitivity decreases at point P1, while increasing at point P2. However, this pattern diminishes as Plate 1's thickness

approaches 1.5 mm. It is interesting that the energy density of point P2 starts to decrease when the thickness of Plate 1 becomes 1.3 mm. Thus, the maximum value of the sensitivity of energy density at point P2 can be expected at h_1 = 1.3 mm.
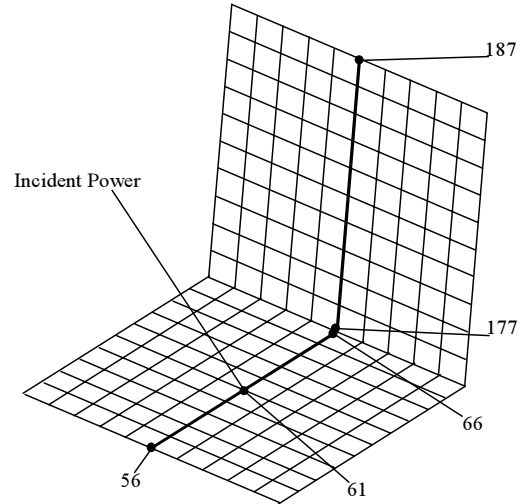

Figure 7 Energy Density Distribution of Two Plates at a Right Angle
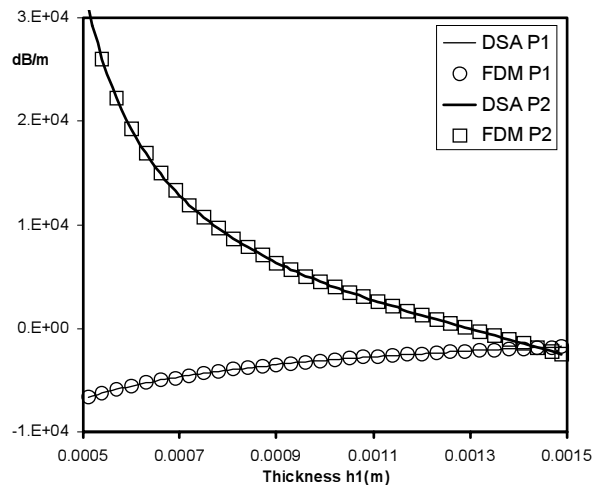

Figure 8 Design Sensitivity Plot of the Energy Density with Respect to the Thickness Design Variable of Plate 1 (2.0 kHz)

Table 2 compares the sensitivity results of energy densities for those nodes along the centerline of the plates (see Figure 7). The same thickness of $h_1 = h_2$ = 1.0 mm is used for both plates. Energy density values are calculated from a frequency average that covers a one-third octave. The first and second columns denote the node number and nodal energy density (performance measure) in dB units, respectively. Performance

9

Table 2 Comparison of Sensitivity Results Obtained from the Proposed and Finite Difference Method ($\theta=90°$, $\omega=2.0$ kHz)

Node	ψ	$\psi'\Delta\varepsilon$		$\Delta\psi$	$\Delta\psi/\,\psi'\Delta\varepsilon\times100\%$	
		DDM	AVM		DDM	AVM
56	0.91237945E+2	0.40465093E-2	0.40465093E-2	0.40473102E-2	100.02	100.02
57	0.91404763E+2	0.24799215E-2	0.24799215E-2	0.24805766E-2	100.03	100.03
58	0.91908154E+2	-0.19791083E-2	-0.19791083E-2	-0.19788282E-2	99.99	99.99
59	0.92790054E+2	-0.89176064E-2	-0.89176064E-2	-0.89178111E-2	100.00	100.00
60	0.94039969E+2	-0.16996344E-1	-0.16996344E-1	-0.16996976E-1	100.00	100.00
61	0.97291986E+2	-0.30821719E-1	-0.30821719E-1	-0.30822884E-1	100.00	100.00
62	0.93991173E+2	-0.17396825E-1	-0.17396825E-1	-0.17397454E-1	100.00	100.00
63	0.92655044E+2	-0.97446228E-2	-0.97446228E-2	-0.97448706E-2	100.00	100.00
64	0.91644878E+2	-0.30619330E-1	-0.30619330E-1	-0.30618179E-2	100.00	100.00
65	0.90977247E+2	0.14228950E-2	0.14228950E-2	0.14231904E-2	100.02	100.02
66	0.90623021E+2	0.32388008E-2	0.32388008E-2	0.32389950E-2	100.01	100.01
177	0.83403422E+2	0.42493917E-1	0.42493917E-1	0.42499934E-1	100.01	100.01
178	0.82417283E+2	0.42846442E-1	0.42846442E-1	0.42852465E-1	100.01	100.01
179	0.81461217E+2	0.43069418E-1	0.43069418E-1	0.43075445E-1	100.01	100.01
180	0.80537757E+2	0.43210071E-1	0.43210071E-1	0.43216100E-1	100.01	100.01
181	0.79655424E+2	0.43298517E-1	0.43298517E-1	0.43304548E-1	100.01	100.01
182	0.78829343E+2	0.43353900E-1	0.43353900E-1	0.43359932E-1	100.01	100.01
183	0.78082023E+2	0.43388322E-1	0.43388322E-1	0.43394355E-1	100.01	100.01
184	0.77443423E+2	0.43409373E-1	0.43409373E-1	0.43415406E-1	100.01	100.01
185	0.76948922E+2	0.43421734E-1	0.43421734E-1	0.43427767E-1	100.01	100.01
186	0.76633956E+2	0.43428182E-1	0.43428182E-1	0.43434215E-1	100.01	100.01
187	0.76525562E+2	0.43430179E-1	0.43430179E-1	0.43436213E-1	100.01	100.01

changes are then recorded for the direct differentiation method (column 3), the adjoint variable method (column 4), and FDM (column 5). Column 5 is the ratio between columns 3 and 5, and column 6 is the ratio between columns 3 and 6. A small design perturbation of $\Delta h = 10^{-3}$ mm is used. In the ratio column (%), results from the two proposed methods are compared with finite difference results). Excellent agreement is observed between the three methods. In fact, sensitivity results from the direct differentiation and adjoint variable methods are the same up to the significant digits shown in the table. Note that the energy density values of the two junction nodes 66 and 177 are different at about 7.2 dB, which confirms the discontinuity of energy density across the junction.

As a final example of parameter design sensitivity analysis, a hysteresis–damping factor is considered as a design variable. Figure 9 compares the sensitivity of energy densities from the proposed method with the finite difference method when the damping factor is the design variable. The effect of the damping factor on the energy density function is always negative for Plate 2. However, such an effect gradually decreases, and shows saturation as the damping factor approaches 0.1. The damping factor's effect on Plate 1 is quite different from its effect on Plate 2. At the very small value of η (0.01 – 0.028), an increase in the damping factor reduces the energy density at Plate 1. However, at a high value the damping factor actually increases the energy density on Plate 1, and its effect is gradually reduced as the damping factor increases.

Energy density's dependence on the damping factor

cannot be generalized because observations in this section depend on excitation frequency, material property, and plate dimensions. However, this example clearly shows that adding more damping material does not always guarantee a reduction in the noise level of structural components. In order to control noise levels, the effects of damping material must be fully understood in each component through design sensitivity analysis.
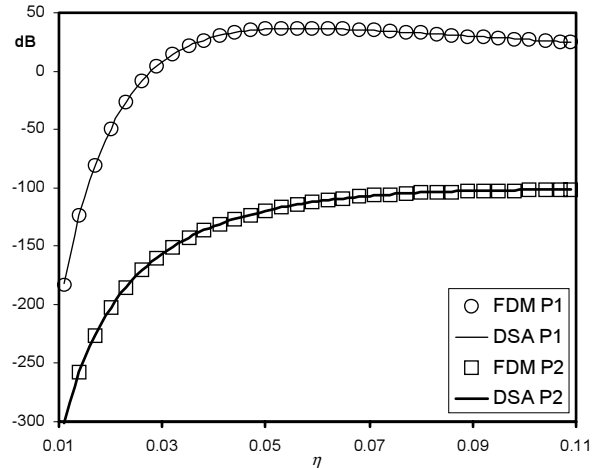

Figure 9 Design Sensitivity Plot of the Energy Density with Respect to the Hysteresis–Damping Factor (2.0 kHz)

5. CONCLUSION

Design sensitivity formulation of the energy finite element method is presented using direct differentiation and adjoint variable methods. Material property, panel

American Institute of Aeronautics and Astronautics

thickness, junction angle, and structural shape are taken into account as design variables, in addition to the hysteresis–damping factor. The continuum approach is used to derive the design sensitivity formulation of the structural component, while the discrete approach is used to obtain the design sensitivity of the junction matrix, required in the coupling of different components. The analytical expression of the power transfer coefficient is differentiated with respect to design variables to obtain the power transfer coefficient sensitivity. Design sensitivity results calculated from the proposed method are compared with finite difference sensitivity results with good agreement. The proposed design sensitivity calculation method is integrated into the design optimization process.

ACKNOWLEDGEMENT

REFERENCE

1. R. R. Salagame, A. D. Belegundu, and G. H. Koopman, 1995, Analytical Sensitivity of Acoustic Power Radiated from Pates, Journal of Vibration and Acoustics **117**(1) 43–48

2. K. K. Choi, I Shim, and S. Wang, 1997, Design Sensitivity Analysis of Structure–Induced Noise and Vibration, Journal of Vibration and Acoustics **119**(2) 173–179

3. J. H. Kane, S. Mauo, and G. C. Everstine, 1991, A Boundary Element Formulation for Acoustic Shape Sensitivity Analysis, Journal of the Acoustical Society of America **90**(1) 561–573

4. D. C. Smith and R. J. Bernhard, 1992, Computation of Acoustic Shape Design Sensitivity Using a Boundary Element Method, Journal of Vibration and Acoustics **114**(1) 127–132

5. K. A. Cunefare and G. H. Koopman, 1992, Acoustic Design Sensitivity for Structural Radiators, Journal of Vibration and Acoustics **114**(2) 179–186

6. D. J. Nefske, J. A. Wolf, and L. J. Howell, 1982, Structural–Acoustic Finite Element Analysis of the Automobile Passenger Compartment: A Review of Current Practice, Journal of Sound and Vibration **80**(2) 247–266

7. R. Lyon, 1975, Statistical Energy Analysis of Dynamical Systems: Theory and Application, The MIT Press, Cambridge, MA

8. F. J. Fahy, 1974, Statistical Energy Analysis: A Critical Review, The Shock and Vibration Digest, 14–33

9. R. Lyon and R. G. DeJong, 1995, Theory and Application of Statistical Energy Analysis (2nd Edition), Butterworth–Heinemann, Boston, MA

10. V. D. Belov, S. A. Rybak, and B. D. Tartakovskii, 1977, Propagation of Vibrational Energy in Absorbing Structures, Soviet Physics and Acoustics **23**(2) 115–119

11. D. J. Nefske and S. H. Sung, 1989, Power Flow Finite–Element Analysis of Dynamic–Systems – Basic Theory and Application to Beams, Journal of Vibration Acoustics Stress and Reliability in Design **111**(1) 94–100

12. J. Wohlever and R. J. Bernhard, 1992, Mechanical Energy Flow Models of Rods and Beams, Journal of Sound and Vibration **153**(1) 1–19

13. O. M. Bouthier and R. J. Bernhard, 1992, Models of Space–Averaged Energetics of Plates, AIAA Journal **30**(3) 616–623

14. P. Cho and R. J. Bernhard, 1998, Energy Flow Analysis of Coupled Beams, Journal of Sound and Vibration **211**(4) 593–605

15. N. Vlahopoulos, L. O. Garza-Rios, and C. Mollo, 1999, Numerical Implementation, Validation, and Marine Applications of an Energy Finite Element Formulation, Journal of Ship Research **43**(3) 143–156

16. R. J. Bernhard and J. E. Huff, 1999, Structural–Acoustic Design at High Frequency Using the Energy Finite Element Method, Journal of Vibration and Acoustics **121**(3) 295–301

17. R. S. Langley and K. H. Heron, 1990, Elastic Wave Transmission through Plate/Beam Junctions, Journal of Vibration and Acoustics **143**(2) 241–253

18. L. Cremer, L Heckel, and E. E. Ungar, 1988, Structure–Bourn Sound, (second edition), Springer–Verlag, Berlin

19. M. Gelfand and S. V. Fomin, 1963, Calculus of Variations, Prentice–Hall, Englewood Cliffs, New Jersey

20. K. K. Choi and E. J. Haug, 1983, Shape Design Sensitivity Analysis of Elastic Structures, Journal of Structural Mechanics **11**(2) 231–269